scientific reports

Check for updates

OPEN

Insights into the pharmaceutical properties and in silico study of novel hydrazone derivatives

Hiba H. Ibraheem[1], Batool K. Queen[1], Matheel D. Al-Sabti[2], Ali A. Issa[1], Yasameen K. Al-Majedy[1], Majid S. Jabir[1]✉, Ghassan M. Sulaiman[1]✉, Buthenia A. Hasoon[1], Merriam M. Eshaq[9], Kareem H. Jawad[3], Sabrean F. Jawad[4], Hayder A. Fawzi[5], Muhammad Shuaib[6], Mazin A. A. Najm[7] & Ayman A. Swelum[8]✉

It has been established that the Hydrazone derivatives have important pharmacological effects. In the first step, hydrazine (NH_2NH_2) reacts with a compound containing a carbonyl group (C = O) in the presence of ethanol and heat, leading to the formation of hydrazone compound (H1). The second step is the formation of the Schiff base (H2) by the reaction of compound (H1) with indole, ethanol, and acetic acid, which contain a double bond (C = N). In the third step, the (H1) reacts with thiophene, ethanol, and acetic acid to form a compound (H3) containing multiple bonds between the indole and thiophene rings. The synthetic test compounds underwent characterization using TLC, IR, 1 H - NMR, and ^{13}C NMR spectral examinations. Both compounds, H2 and H3, exhibit antioxidant activity at different concentrations (from 12.5 to 100 μgmL^{-1}), where the effect increases gradually with the increase in concentration. The compounds (H2 and H3) exhibited an apparent inhibitory effect on the growth of *Staphylococcus aureus*, *Escherichia coli*, and *Candida albicans*. Calculations have been performed for DFT, molecular docking, molecular dynamics simulations, and the ADMET protocol, and they are essential for describing the interaction and stability. In hydrazone derivatives, groups like amine, hydroxy, thiophene, and indole form hydrogen bonds and electrostatic interactions with amino acids such as arginine, lysine, glutamic acid, and aspartic acid. These interactions are crucial to evaluating the compound's stability and its potential to inhibit enzyme activity. The results indicate that the compound shows strong binding and stability at the active site, making it a promising candidate for further studies as an anti-colon cancer agent.

Keywords Hydrazone, Antimicrobial, Antioxidant, Homo-LUMO, Docking study, Anticancer

Compounds with the imimine group (> C = N-), commonly called hydrazones, are created by condensing hydrazides with active carbonyls. In medical and pharmaceutical chemistry, Schiff bases have acquired significance in pharmaceutical and medical fields, which were imputed to their biological activities such as anti-inflammatory[1], analgesic, antibacterial, anticonvulsant[2], antitubercular, antitumor, scavengers and anthelmintic. The imine group in the Schiff base molecule has the ability to form a hydrogen bond with the cell constituents' active centers and interferes in processes of normal cells[3]. Hydrazones have specific characteristics that make them a viable option for designing novel molecules. They have a functional nitrogen electron pair and a conjugated C = N bond. Their two interconnected nitrogen atoms set them apart from other members of the same class (imines, oximes)[4]. When these nitrogen atoms are combined with carbon, which is both electrophilic and nucleophilic, hydrazones with various functional groups are formed, which gives rise to products with distinct biological properties[5]. A member of the heterocyclic compound family, indole has two rings: a fused five-membered pyrrole ring and a six-membered benzene ring[6]. Typically, hydrazides are heated

[1]Department of Applied Sciences, University of Technology, Baghdad, Iraq. [2]College of Science, Uruk University, Baghdad, Iraq. [3]Department Laser and Optoelectronics Engineering, University of Technology, Baghdad, Iraq. [4]Department of Pharmacy, Al-Mustaqbal University, Hillah 51001, Iraq. [5]Department of Pharmacy, AL Mustafa University, Baghdad, Iraq. [6]Key Laboratory of Animal Breeding Reproduction and Molecular Design for Jiangsu Province, College of Animal Science and Technology, Yangzhou University, Yangzhou 225009, China. [7]Department of Pharmacy, Mazaya University College, Nasiriyah, Iraq. [8]Department of Animal Production, College of Food and Agriculture Sciences, King Saud University, Riyadh 11451, Saudi Arabia. [9]Department of Biomedical Engineering, University of Technology, Baghdad, Iraq. ✉email: 100131@uotechnology.edu.iq; ghassan.m.sulaiman@uotechnology.edu.iq; aswelum@ksu.edu.sa

with various aldehydes in solvents like acetone or ethanol to create hydrazones, a process that can be readily verified by looking at the spectrum data. The current research project is aimed at creating biologically active derivatives with potential antioxidant and antimicrobial properties by synthesizing new hydrazone derivatives of 3-hydroxybenzohydrazide and thiophene-2-carbohydrazide with 1 H-indole-3-carbaldehyde, based on the previously mentioned literature. Figure 1 below shows the acyl hydrazone structure. These computational strategies can be used to investigate the chemical and biological properties of the H2 and H3 compounds. These analyses help discover how molecular modifications affect the activity and efficacy of the compounds as potential drugs and predict how they interact within biological systems[7]. Therefore, the aim of present work is to synthesize and characterize novel hydrazone derivatives through multi-step reactions, including forming Schiff bases and indole-thiophene linkages, and to evaluate their pharmacological activities, specifically antioxidant and antimicrobial properties. Additionally, computational methods such as density functional theory (DFT), molecular docking, molecular dynamics simulations. ADMET protocol also used to assess thecompounds' stability, enzyme inhibition potential, and suitability as promising candidates for anti-cancer studies, particularly against colon cancer.

Procedure and technique

Chemicals and apparatus

Dimethyl sulfoxide (DMSO), crystal violet stain, methanol, 3-hydroxybenzaldehyde, and 1-indole-3-carbaldehyde were acquired from Sigma-Aldrich (Germany). 3-hydroxybenzohydrazide was purchased from Merck, Germany. The UV/VIS spectra were measured using a Lambda 19 spectrophotometer from PerkinElmer (Waltham, MA, USA). Muller-Hinton agar media was purchased from Mast, Liverpool, England. Analytical grade reagents and chemicals were all that were required. The melting points of the synthesized compounds

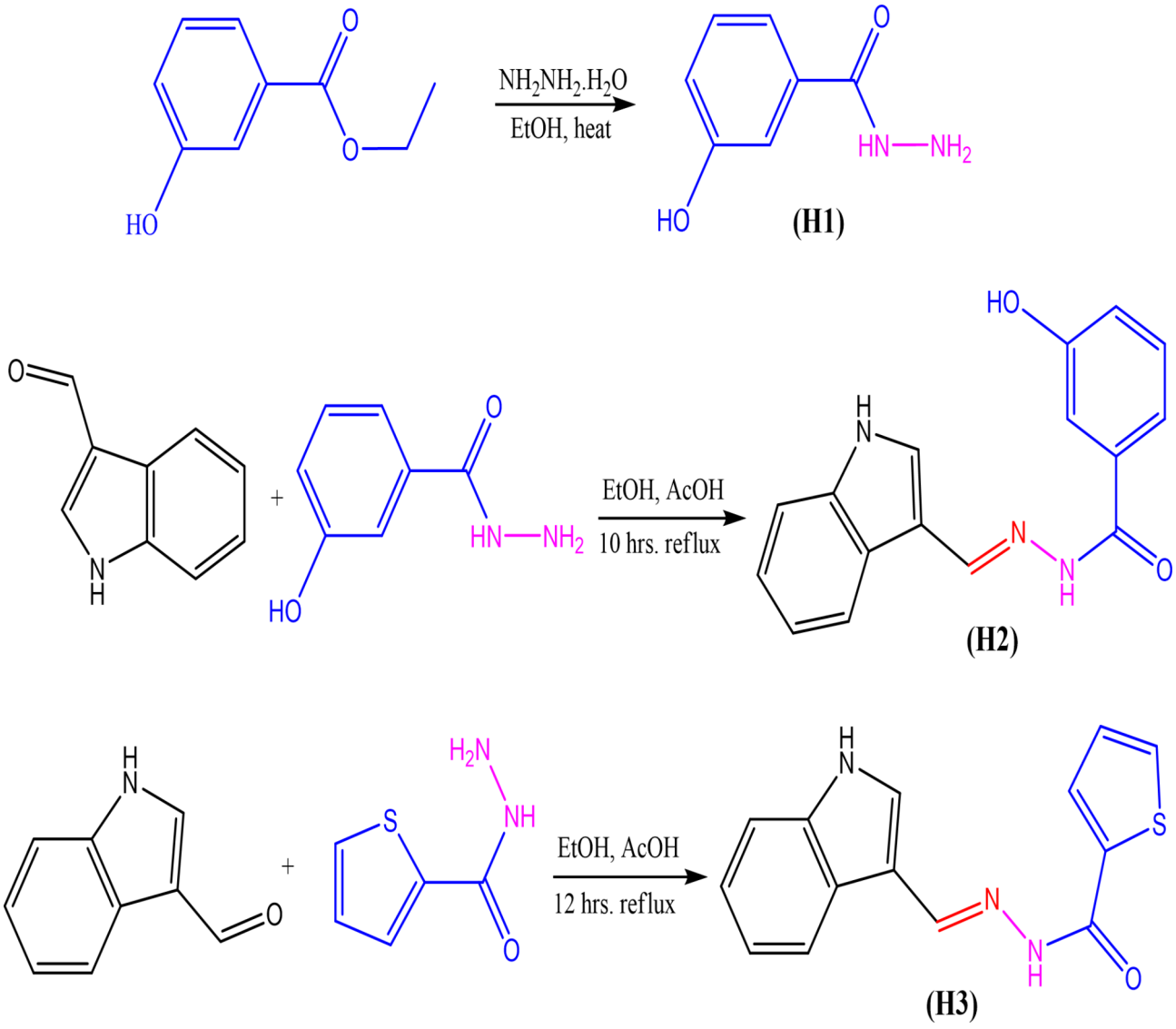

Fig. 1. The synthetic compounds' reaction sequences (**H1–H3**).

were determined using a Gallenkamp MF B600 010 F melting point apparatus. Infrared spectra were recorded on a Shimadzu FTIR-8400s spectrophotometer (Japan), with the frequencies expressed in cm^{-1}. The 1 H-NMR spectra were recorded on BRUKER Ultrashield 500 Plus spectrometer from Germany with DMSO-d_6 as the solvent, and the chemical shifts are reported in δ ppm. The molecular structure was drawn by ChemDraw Ultra 2011 edition. The FT-IR spectra were recorded on a Nicolet 380 FT-IR spectrometer using potassium bromide pellets supplied by Thermo Electron Corporation. The 1 H-NMR spectra were carried out on BRUKER 500 MHz spectrometer, with tetramethylsilane as the internal standard and DMSO-d_6 as the solvent. After extraction, drying of all the organic layer was performed over sodium sulfate. The FT-IR, 1 H-NMR, and 13 C NMR data of compounds H2 and H3 are given in the supplementary data file (Supplementary Figs. 1–4). All reagents and solvents used were of analytical grade, unless stated otherwise.

Microorganisms

The synthesized compounds were tested for their antimicroial activities against clinical isolates of *Staphylococcus aureus* (*S. aureus*), *Escherichia coli* (*E. coli*), and *Candida albicans* (*C. albicans*). Microorganisms were obtained from the Medical Microbiology Laboratory, Biotechnology Division, Department of Applied Science, University of Technology, Baghdad, Iraq. The isolates were speciated using the VITEK2 system (BioMerieux, USA).

Compounds synthesis

Step 1: Compound (H1): The following 3-hydroxybenzohydrazide (H1) compound was prepared by the method previously described[8] as seen in Fig. 1.

Step 2: Compound (H2): 3-hydroxybenzohydrazide (H1; 0.005 mol), 1 H-indole-3-carbaldehyde (0.005 mol), 30 mL of chloroform-methanol (1:1v/v) combination and 1 mL of glacial acetic acid were refluxed in a water bath for three hours. The separated material was filtered and given an additional dosage of methanol wash after the mixture was allowed to cool[9].

Step 3: Compound (H3): For four hours, a mixture of 1 H-indole-3-carbaldehyde (0.005 mol), 1 mL of glacial acetic acid, and thiophene-2-carbohydrazide (0.005 mol) in a 30 mL chloroform-methanol (1:1v/v) mixture were refluxed in a water bath. The separated material was filtered after letting the mixture cool and washed with an extra dose of methanol[10].

Isolation of microorgansims

The isolates were collected under sterilized conditions, inoculated on nutrient agar, and incubated for 48 h for fungus and 24 h at 37 °C. Isolates were grown overnight in nutrient broth for 18–24 h at 37℃ to adjust suspended cells to 0.5 McFarland standards. The isolated microbes were identified using the VITEK 2 system with a (GP) card for gram-positive bacteria identification, a (GN) card for gram-negative bacteria identification, and a (YST) card for fungal identification.

Antimicrobial activity

The microorganisms of each isolate were cultured and then plated out on Mueller-Hinton agar and SDA agar media. Each strain of bacteria was equally distributed across each plate using clean cotton swabs. After that, five wells were used for different compound concentrations, while six wells served as a control. The six wells had a diameter of 6 mm and were created using gel punctures on the agar feed plates. The concentrations were 12.5, 25, 50, 75, and 100 μgmL^{-1}. Distilled water (DW) was used as a control to dissolve the compounds and evaluate the chemical compounds' impact. Each hole filled with 50 µL of the produced compound using a micropipette. The inhibitory zone diameter for each hole was measured in millimeters on average during three experiments after the plates were cultured for 48 h for fungus and 24 h at 37 °C[11].

Antioxidant activity by DPPH radical

The solution was prepared by dissolving 0.004 mg of DPPH in 100 ml of absolute ethanol in a volumetric flask. Then, shake well using a vortex and wrap in aluminium foil to prevent photo-oxidation. 0.5 mg of ascorbic acid (Vitamin C) dissolved in 100 mL of a 1:1 (Ethanol: D.W.) as a positive control with a few modest modifications, the antioxidant activity of various synthesis products was assessed. The 1, 1-Diphenyl-2-picryl-hydrazyl (a stable DPPH radical) was used to evaluate the scavenging activities of compounds, which were evaluated at 12.5, 25, 50, 75, and 100 μgmL^{-1}. 75 µL of synthesis compound samples (for each sample) were combined with 925µL of DPPH solution that had been previously made. The negative control was combined with 925 µL of ethanol and 75 µL of DPPH. There were 75 µL of ascorbic acid and DPPH for the positive control. Before measuring the optical density (OD) at 517 nm, the test samples and controls were shielded from light and allowed to sit at room temperature for 30 min. Which was calculated using Eq. (1):

$$\text{Scavenging evaluation } \% = \left[\left(\text{OD}^{\text{control}} - \text{OD}^{\text{sample}}\right)/\text{OD}^{\text{control}}\right] \times 100 \quad (1)$$

OD control is the absorption of control, and the OD^{sample} is the absorption of the tested extract solution.

Quantum and reactivity parameters

The most pertinent characteristics are global reactivity indices obtained from the theoretical density functional theory (DFT). They have crucial characteristics that help us comprehend compounds' kinetic stability and chemical reactivity. The energy of the lowest unoccupied molecular orbital (ELUMO) and the energy of the highest occupied molecular orbital (EHOMO), energy gap (ΔE), chemical potential (μ), chemical hardness (η), chemical softness (S) and nucleophilicity (N), ionization potential (I), and electron affinity (A) are the descriptors of global reactivity[12]. The following formulas were used at B3LYP/6-311G to calculate

the descriptors: ($\Delta E = E_{LUMO} - E_{HOMO}$), ($S = 1/2\eta$), ($\omega = \mu^2/2\eta$), ($\mu = E_{LUMO} + E_{HOMO}/2$), ($\eta = E_{LUMO} - E_{HOMO}/2$), ($S = 1/(2)$), ($N = E_{HOMO}$ (Nucleophile) $+ E_{HOMO}$) (TCE)), ($I = -E_{HOMO}$), ($A = -E_{LUMO}$In this investigation[13], . MEP analysis was conducted to identify the key nucleophilic and electrophilic sites within the optimized structures.

ADMET protocol

SwissADME, an open-source web-based program, may be used to generate ADMET parameters and examine the drug-like effects of H2 and H3 in silico (H2 and H3). This concerns the format of SMILE. Using pkCSM graph-based signatures, the theoretical interpretations of the ADMET features were previously described, predicting the small compounds' potential as drugs. Furthermore, physicochemical indices can control the Lipinski rules by controlling medication absorption and diffusion[14].

The molecular docking strategy

Docking studies were performed using the selected target protein for antibacterial activity. A study was conducted on the amino acids associated with colorectal cancer (CRC; ID: 7ZWA) obtained from the Protein Data Bank (https://www.rcsb.org/structure/7ZWA). At a resolution of 2.80 Å, it is considered suitable between the angle range of 1.5 and up to 2.5 in docking studies[15]. In both docking runs, the ages used to analyze interactions between docked poses were correctly set, and 0.4 Å of RMSD was found in every case concerning crystal structure, which indicates a reasonable score for our ligand. These are typical criteria for validating molecular docking results, stating that low energy (-7 kcal/mol or even lower) and RMSD values should be kept around 2Å for a reliable outcome. To investigate the strengths of interaction and any conceivable theoretical association with its experimental antibacterial activity, each of these compounds (H2, H4, and PO_4 referance) was docked into the active % site provided by the receptor. The docking simulations, keeping PO_4 as a reference ligand, were carried out using the Molecular Operating Environment (MOE) software under standard conditions. The receptor protein was processed with MOE while retaining water molecules in the active site to help towards hydrogen bonding with ligand and target. The protein structure with gaps caused by the diffraction of the protein was fixed and protonated. Optimization was followed using the Assisted Model Building with Energy Refinement (AMBER 10) program and extended Hückel Theory (EHT)[16].

Molecular dynamics simulations

One of the isothermal-isobaric molecular dynamics formalisms, a real-time Hamiltonian formulation for NPT simulations with one additional Poincaré time transformation in original Nosé-Andersen (NA) Hamiltonian. DESCRIPTIONS: This methodology was utilized to receive descriptions of the molecular dynamics (MD) BoM ligands. The optimal system setup included MMFF94x force field, a sphere boundary type, water as solvent and 6 margin setting (and FACTS). Solvent molecules were bistripped taking out all the waters further than 4 Å. The simulation was performed for 1500 ps with a time step of 0.002 ps, initially equilibrated at T = 300 K for 100ps before the simulations. When NPA calculations were performed, constraints on light bonds had to be enforced to achieve accuracy.

Maintenance of cell cultures

HT-29 cell lines were cultured in RPMI 1640 medium containing 10% fetal bovine serum and penicillin/streptomycin. The cells were passaged twice weekly at 80% confluence using Trypsin-EDTA for detachment and kept in an incubator at 37 °C.

Cytotoxicity assays

For the cytotoxic effects of H2 and H3, an MTT assay was conducted in 96-well plates. (MTT) assay was done for the quantification of HT-29 cell viability. At density of 1×10^4 cells per well were seeded in 96-well plates in a complete medium and allowed to adhere for 24 h. The cells were then treated with H2 and H3 at different concentrations. After 24 h, 48 h, and 72 h of incubation, MTT stain was added at a concentration of 2 $mgmL^{-1}$ according to the standard protocol. The absorbance at 490 nm (OD490) was measured using a microplate reader[17]. The cytotoxicity was calculated according to equsion below.

$$\text{Cytotoxicity } (\%) = A - B/A \times 100 \quad (2)$$

Where A represents the optical density of the control, and B represents the optical density of the samples.

Acridine orange–ethidium bromide staining

Acridine Orange (AO) and Ethidium Bromide (EtBr) dye were mixed at a concentration of 10 μg mL^{-1} in PBS and then used to stain HT-29 cells after being treated with H. The samples were then visualized by fluorescence microscopy. The living cells were green in colour and carried a normal nuclear structure, while apoptotic cells were Orange-Red in colour and had a condensed or broken nucleus[18].

Statistical analysis

The collected data were statistically analyzed using an unpaired T-test in GraphPad Prism 6. Three separate measurements' means and ± SDs were displayed, together with a significant P-value of $P < 0.05$[19].

Results and discussion

Characterization of compounds H2 and H3

The FT-IR spectra were recorded on a Thermo Nicolet 380 FT-IR spectrometer using KBr pellets. General: ^{1}H-NMR spectra were recorded on a Varian 300 MHz spectrometer using tetramethylsilane (TMS) as an internal standard, and DMSO-d_6 was used as a solvent. After the extraction, all organic extracts were concentrated and dried over sodium sulfate. The FT-IR, ^{1}HC-NMR and ^{13}C NMR spectroscopic data of synthesised compounds (H2, H3) are given in the supplementary document. Reagents and solvents were of commercial grade unless otherwise indicated. This data includes compound (E)-N'-((1H-indol-3-yl)methylene)-3-hydroxybenzohydrazide[18] (H2): Yield 80%, Mp.: 233–235 °C., Chemical Formula: $C_{16}H_{13}N_3O_2$, Molecular Weight: 279, IR (KBr) cm^{-1}: (1608 C = N imine), (3209 N-NH). ^{1}H-NMR (500 MHz, DMSO-d6) δ ppm: 11.55 (s, NH), 11.33 (s, N-NH), 10.06 (s, OH), 8.57 (s, N = CH), 8.31–6.83 (m, 9 H, Ar-H and indole ring). ^{13}C NMR (106.2), (112.31), (115.40), (119.01), (120.75), (122.53), (123.04), (124.81), (129.90), (130.44), (137.46), (137.67), (144.54), (155.54), (160.77), (162.67).

(E)-N'-((1H-indol-3-yl) methylene) thiophene-2-carbohydrazide (H3): Yield 72%; M.P.: 264–266 °C, Chemical Formula: $C_{14}H_{11}N_3OS$, Molecular Weight: 269, IR (KBr) cm^{-1}: 3213 (NH), (1627 C = O), (1604 C = N). 1512 (C = C); ^{1}H- NMR (500 MHz, DMSO-d6): 11.62 (s, NH), 11.57 (s, N-NH), 8.43 (s, N = CH), 8.10–7.14 (m, 9 H, Ar-H, indole ring and thiophene ring). ^{13}C NMR (111.69), (112.52), (120.89), (121.07), (122.44), (127.17), (128.65), (130.91), (131.58), (134.22), (137.51), (139.54), (145.33), (161.13).

Antimicrobial activity

The well inhibition zone diameters were used to measure the antibacterial activity. The good diffusion results against both positive (+ ve) and Gram-negative (-ve) bacteria are displayed in Figs. 2 and 3, and also shown in supplementary Figs. 5 and 6. Antimicrobial studies conducted in vitro revealed that the molecules generated in Fig. 1 exhibit strong inhibitory effects on *E. coli*, *S. aureus*, and *C. albicans*[20]. There's a low effect of the synthesis compound on the growth of *E. coli*, but its effect varies on the bacteria and *C. albicans*. For compound H2, the highest effect was observed against *S. aureus*, which had a zone of inhibition of 25 ± 0.01 mm, followed by *C. albicans* (23.33 ± 0.21 mm) and then *E. coli* (14.4.±0.12 mm). For compound H3, the highest effect was observed against *S. aureus*, which had a zone of inhibition of 24 ± 0.01 mm, followed by *C. albicans* (22 ± 0.11 mm) and then *E. coli* (11.50 ± 0.11 mm). The derivatives, compounds H2 and H3, showed activity against *Candida albicans* due to their respective Hydrazone derivatives have been shown to exhibit antimicrobial characteristics. The benefit of this method is that it can identify and measure antibiotics without requiring costly instrumentation or derivatization. Furthermore, the synthesized compound derivatization enhances antibiotic penetration into bacterial cells. There were 12 hydrazide hydrazone 5a–l derivatives made. The chemical structure was confirmed by elemental analysis and spectral studies. An assessment of the synthesized compounds' antibacterial properties revealed that compounds 2, 5a, 5c, 5d, and 5f had significant effects on tested bacterial strains. The most active inhibitory zone was hydrazide hydrazone 5f, with widths ranging from 16 to 20.4 mm. Furthermore, an evaluation of the minimum inhibitory concentration (MIC) was conducted. The results obtained with hydrazones 5c and 5f were the best. The MIC of 5c for *B. subtilis* was 2.5 μgmL^{-1}. The MIC of 5f for *K. pneumoniae* and *E. coli* was 2.5 μgmL^{-1}. Using a molecular dynamics simulation analysis of the most active chemicals, 5f and 5c, binding free energies were calculated using the molecular mechanics-generalized born surface area (MM/GBSA). Additionally, computational studies showed that 5f had a significant affinity for DNA gyrase B's active region, indicating that this molecule may provide a solid foundation for future structure-based design creativities[21].

Anti-oxidant activity

The DPPH assay quantifies the hydrogen-donating capacity of chain-breaking antioxidants that can provide free radicals with H+, resulting in a harmless type and inhibition of the lipid oxidation propagation point. Theantioxidant action as a DPPH + radical scavenger is caused by a decrease in these radicals (Fig. 4), which depicts the properties of the synthesized molecules (H2 and H3) that scavenge free radicals. Thus, synthesized molecules demonstrate their capacity to interact with and neutralize free radicals, thus averting any potential harm. In the industrial world, antioxidants are also widely used as food and cosmetic preservatives. The antioxidant properties of synthesized chemical compounds at different doses (12.5, 25, 50, 75, and 100 μgmL^{-1}) are shown in Fig. 4. Variations in these chemicals' antioxidant capabilities are evident from the data. A deeper look at the concentrations reveals that the synthesized compound dramatically and concentration-dependently lowered the levels of DPPH. Notably, Fig. 4 illustrates that compound H2 had the highest DPPH radical scavenging activity at 86.33%. There is a hydroxyphenyl ring in this material. Compound H2 having these substituents is expected to exhibit antioxidant activity. When reactive oxygen species are present, oxidation can damage a wide range of biomolecules. Moreover, it has been demonstrated that compounds found in nature have antioxidant properties[22]. Compound (H3) showed the maximum antioxidant activity, reaching 82.00%, at a concentration of 100 μgmL^{-1}. Control has an antioxidant activity of 95%, in contrast because it containe NH-group in their structure. This is significant because antioxidants are essential in giving reactive radicals an electron so they can become more stable and non-reactive species[23]. Twelve new isonicotinic hydrazide-hydrazone analogues were created. Spectroscopic methods have been used to characterize the new compounds' structures. From 21.00 to 59.48%, all substances have demonstrated inhibitory actions against the AChE enzyme. At a dose of 0.1 mM, compound 5 has demonstrated the highest inhibitory action against AChE, with a 59.48% efficacy. Furthermore, FRAP and DPPH tests were conducted to ascertain the efficacy of the new compounds as antioxidants. Compounds 1–12 have FRAP values ranging from 26.989 to 3415.556 µmol $FeSO_4.7H_2O$/mg. Additionally, in DPPH radical scavenging activities, they demonstrated moderate antioxidant potential in the range of SC50 = 0.03–87.32 μgmL^{-1}in comparison to the control Trolox (SC50 = 0.004)[24].

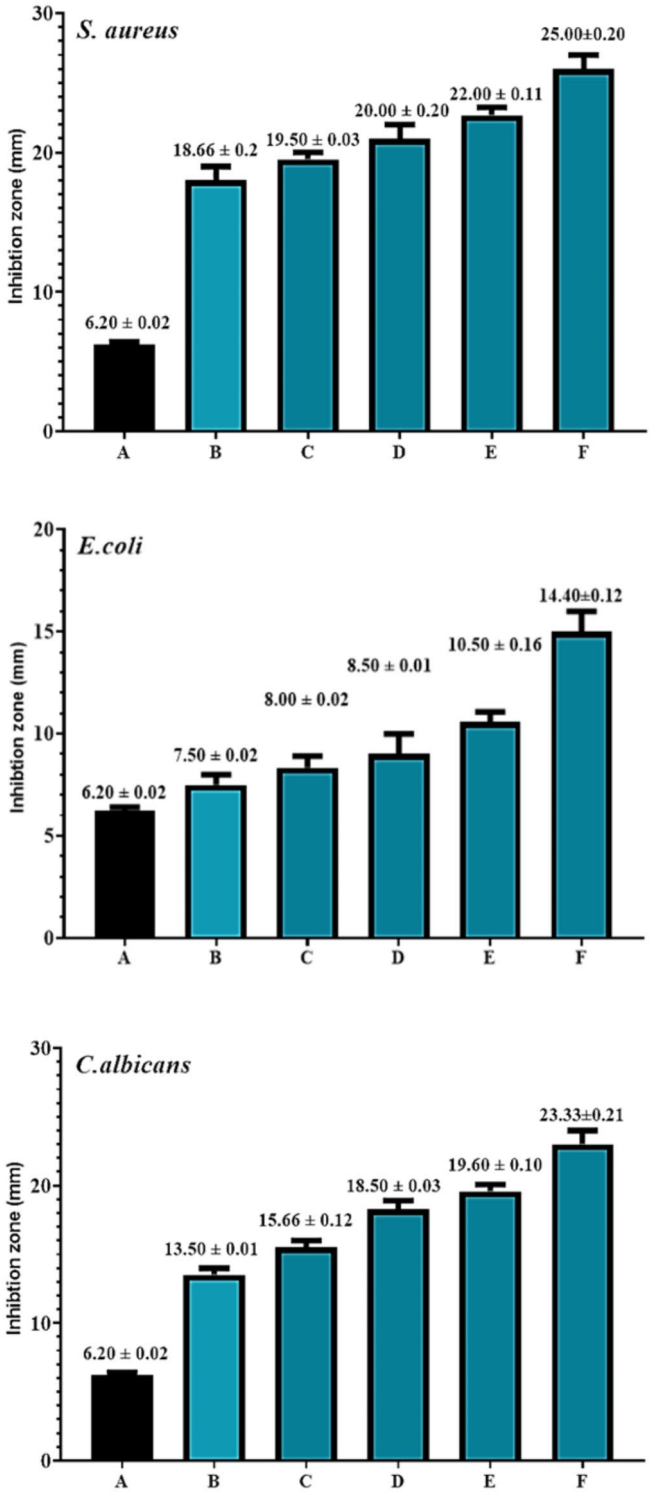

Fig. 2. Antimicrobial activity of synthetic compound (H2) against *Staphylococcus aureus*, *Escherichia coli*, and *Candida albicans*. A = control. B = 12.5 μgmL^{-1},C = 25 μgmL^{-1},D = 50 μgmL^{-1},E = 75μgmL^{-1}, and F = 100 μgmL^{-1}.

Antioxidant mechanisms of compounds H2

The suggested antioxidant mechanism for the synthetic molecule H2 is based on the hydroxyl (in its enol form) hydrogen atom, which was influenced by inductive effects and character. The molecule becomes more stable when hydrogen is released more easily due to resonance and inductive effects[25]. Due to the stability of its free

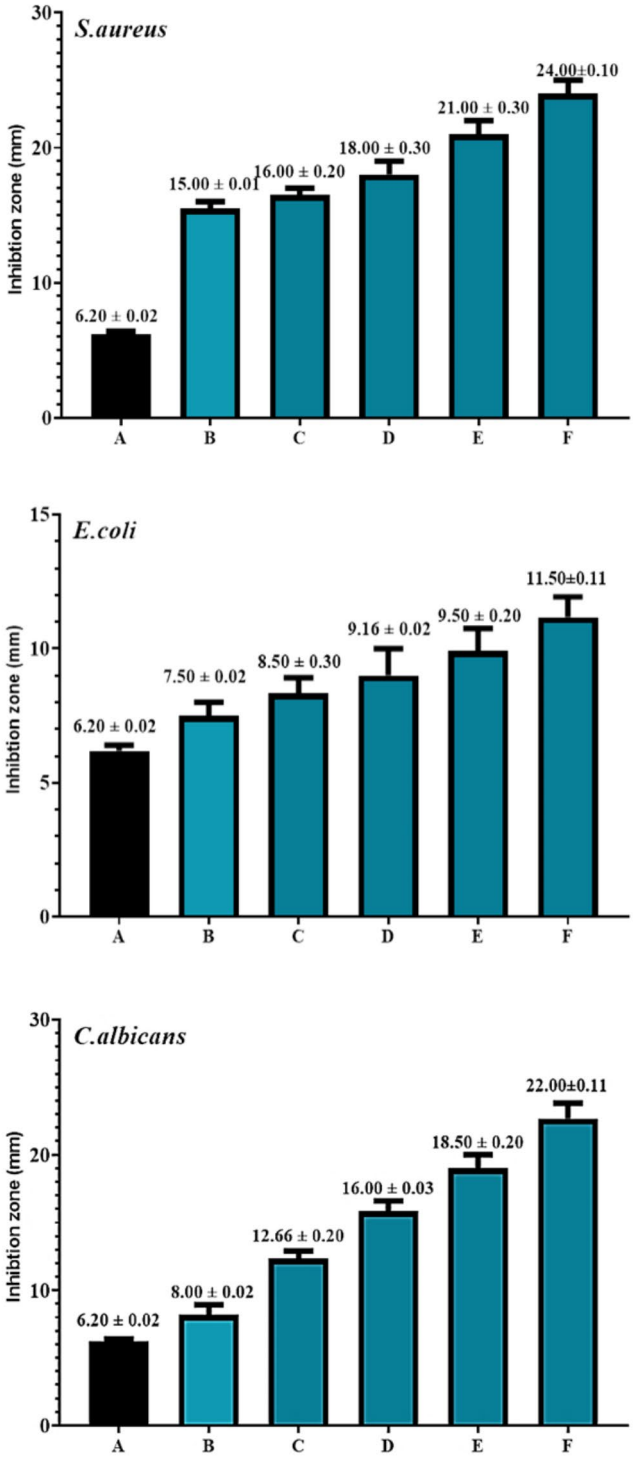

Fig. 3. Antimicrobial activity of synthetic compound (H3) against *Staphylococcus aureus*, *Escherichia coli*, and *Candida albicans*. A = control. B = 12.5 μgmL^{-1},C = 25 μgmL^{-1},D = 50 μgmL^{-1},E = 75μgmL^{-1}, and F = 100 μgmL^{-1}.

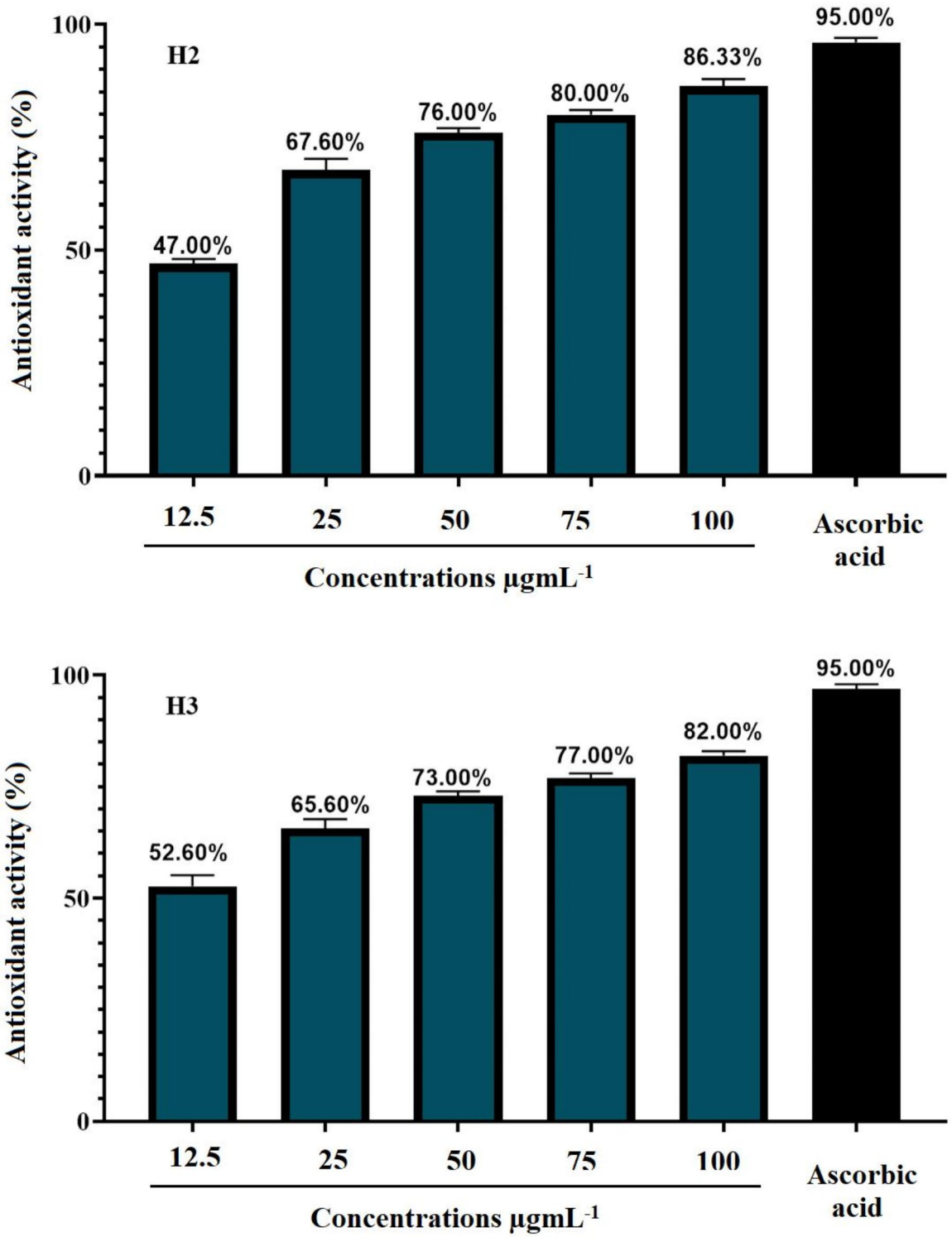

Fig. 4. Antioxidant activity of synthetic compounds H2 and H3.

radical intermediates, compound (H2) possesses scavenging properties. Hydrogen atoms can be easily separated from hydroxyl (enol form)[26].

Quantum and reactivity parameters

The quantum and reactivity parameters were calculated and presented in Table 1. FMOs are distributed electronically for the optimum chemicals (H2, and H3), as shown in Fig. 5 and obtained from Gauss. The results of global hardness and softness are related to the stability of the chemical system and the resistance of a molecule

Molecules	Total energy a.u.	E_{HOMO} eV	E_{LUMO} Ev	Gap energy eV	I eV	A eV	η eV	σ eV	χ eV	μ eV	ω eV	D (deby) eV
H2	− 932.743	− 6.0240	− 3.0400	2.984	6.0240	3.0400	1.492	0.335	2.6318	− 4.5320	4.0375	5.4206
H3	− 1178.276	− 5.9674	− 2.9679	2.999	5.9674	2.9679	1.499	0.333	2.6884	− 4.4677	4.4677	3.5513

Table 1. The HOMO and LUMO energies, energy gap (ΔE), and global reactivity indices (μ, χ, η, ω, A, I, σ, N) were assessed for the compounds H2 and H3. − 8.6559 eV is the HOMO energy. At DFT/B3LYP 6–31 G, the reference system (TCE) had been computed.

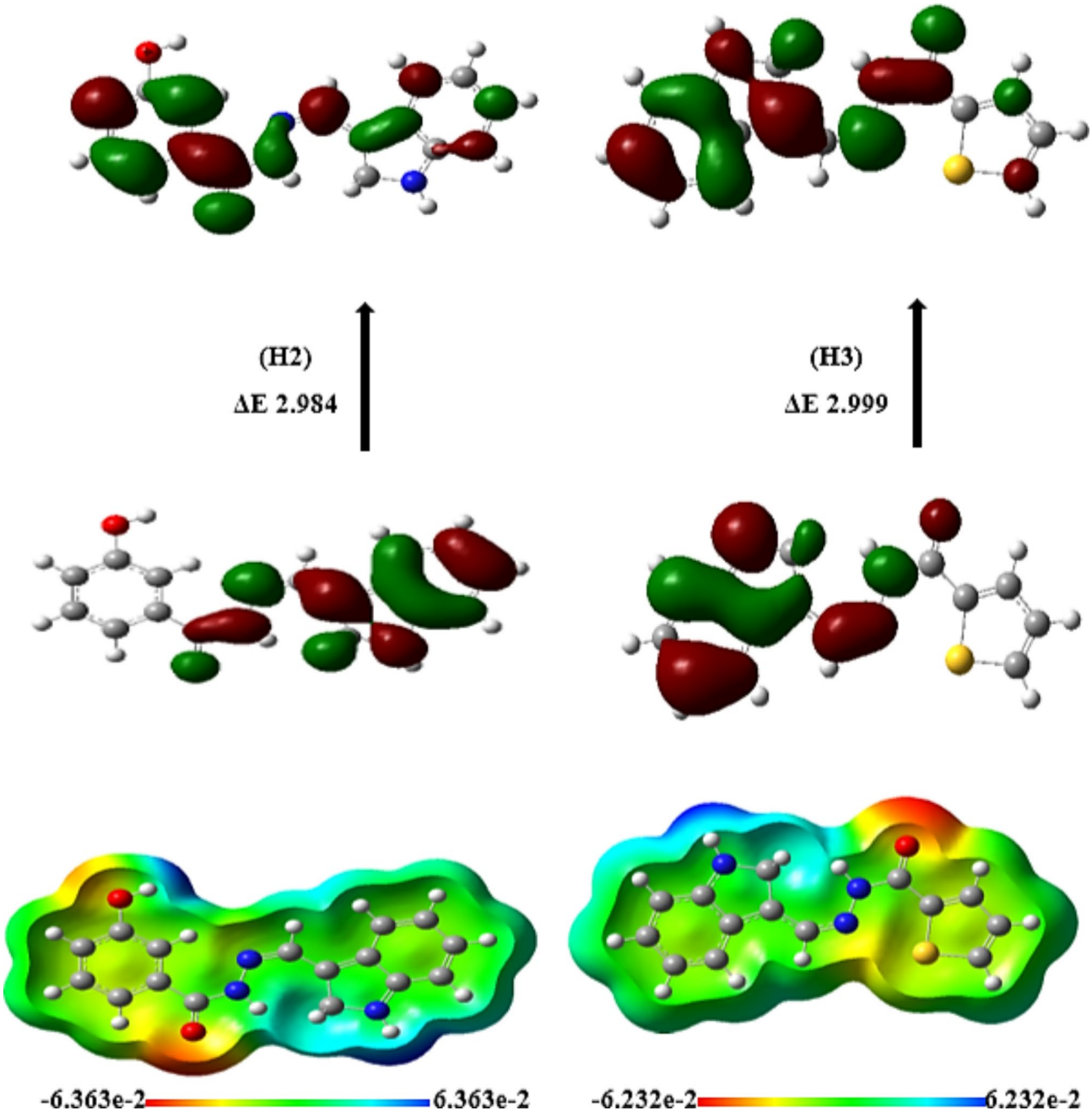

Fig. 5. FMOs for the optimized compounds H2 (**A**) and H3 (**B**) are distributed electronically.

to changes in electron density. Molecules with higher hardness are generally more stable and less reactive[27]. This information is valuable in pharmaceutical manufacturing to ensure the stability of drug compounds during synthesis and storage, as shown in Table 1, indicating that H2 and H3 compounds. In addition, H2 and H3 have a smaller energy gap (ΔE = 2.984 eV and 2.999 eV), are more stable and more reactive (ΔE) 36, considered an important factor in drug design, the selection of molecules with specific electronic properties can affect their reactivity and interactions with biological targets. The electronic chemical potential (μ) for H2 and H3 (μ = -4.5320 eV and − 4.4677 eV) is a measure of the tendency of a system to exchange particles with its surroundings. It can be important in processes involving the transfer of electrons or other charged species[28]. We classified organic molecules into marginal nucleophiles ($N < 2.0$ eV), moderate nucleophiles (2.0 eV $\leq N \leq$ 3.0 eV) and strong nucleophiles ($N >$ 3e V) by analyzing typical kind of simple deposited polar organics used in nature(ulfilling the constant control). This is illustrated using the benchmark tetracyanoethylene (TCE) which has a lowest EHOMO over any of those studied. On the basis of that classification, we might consider compounds H2 and H3 to be marginal nucleophiles even though Table 1 considers these guys solid strong. Electrophilicity (ω) is a good indicator to investigate reactivity of organic compounds in polar reactions and the most electrophilic sites for H2, H3 with ω = 4.0375 eV & 4.4677 eV are fundamental properties to understand and predict reaction mechanisms[30]. Nucleophilicity and electrophilicty properties of reactants are important when performing chemical transformations in pharmaceutical manufacturing. Molecular Electrostatic Potential (MEP) can define the most important electrophilic and nucleophilic zones on molecular surface. A color–coded map of the potential range on the surface is given in Fig. 5, wherein red represents sites that react most easily (e.g., due to cavities). Oxygen (red scale), and the thiophene group were considered to be good nuclueophiles e.g. NO2 on nitrogen can push more electron desnity into ring. In contrast, the indole ring region (blue scale) has a low electron density; hence easier to lose hydrogen and forms resonant structures.

ADMET protocol and drug-likeness prediction

Five determinants can be used by the Lipinski rules to evaluate the validity of the drug properties in the studied compounds: a molecular weight of less than 500 Da and a high lipophilic property, such as a partition coefficient LogP value of less than 5, H-bond donors less than 5, H-bond acceptors less than 10, as well as a molar refractivity value ranging from 40 to 130. When more than two of these criteria are met, the investigated molecule may exhibit characteristics similar to those of a medication. The bioavailability score, which was more relevant for H2 and H3 substances, was identified with the considerable assistance of other filters, including Ghose, Veber, and Egan for the study. The clarified pharmacokinetic and drug-likeness parameters for the investigated substances are shown in Table 2. The availability of a drug for high percentage partitioning in gastrointestinal cells, like H2 and H3, which mimic the control action, is another aspect of pharmacokinetic features. The study's proportionate distribution of the molecules, wherein the present (H2 and H3) are distributed in the blood of humans, is indicated by the blood-brain barrier (BBB) parameter. Five cytochrome P450-related enzymes (CYP1A2, CYP2C19, CYP2C9, CYP2D6, and CYP3A4) can be used to determine a compound's propensity to block. This characteristic plays a critical role in toxicity and other adverse drug reactions[31].

Molecular docking strategy

A bio-complexed system's efficacy depends on the affinity and interaction mode between ligand-protein contents. The calculated total binding energies and the relative interaction types between ligands (H2, H4, and PO_4) and target protein with colorectal cancer (CRC; ID: 7ZWA) simulation are given in Table 3. Also, the binding energies for H2 and H3 (-5.6203, -5.4409 kcal/mol) got my attention because they were shown to have a better bonding potential than the control ligand PO_4 (-3.34019 kcal/mol)[32]. Figures 6 and 7 show superimposed structures of the studied ligands with control PO_4 inside the predicted active site and strong conventional hydrogen bonds and carbon-hydrogen bonds of different bio-complexe conformers. Additionally, within each complex, the type of interaction depends on which amino acid from these sites interacts: ASP79 or GLU250. At the same time, non-covalent interactions, including π-π T-shaped and offset stacking with phenyl ring of ligands, work as a glue between activation site amino acids, namely GLU250, ASP81 but also bridge other potential interaction sites like hydrophobic clusters, Lys90(exterior), ASP79(interior); ARG252;10 in protein. Recipe landscape. These π-anion and π-cation type non-covalent interactions are also attached to P-O bonds, which merge with the δ-bonds of an aliphatic amine than control (PO_4). On the contrary, some unfavourable bumps with bacterial enzymes in the docked control complex may lead to instability. These positive interactions aid in upholding biocomplexity even with the negative ones. Furthermore, the stability of this complex in the active site is reinforced by van der Waals interactions arising from the distribution of some amino acids to inhibitor surfaces[33].

Simulations of molecular dynamics

The constancy and stability of the binding affinities of the two most promising inhibitors' docked receptor ligands were determined using MD simulations. Chemicals (H2 and H3) were examined in further detail. The stability of the two receptor-ligand pairs throughout time is seen in Fig. 8. The two compounds ranged between 0 and 1500 s before stabilizing, and they maintained their stability throughout the simulation process while displaying the same designs.

H2, and H3 induce cytotoxicity in HT-29 cells

The cytotoxic effect of H2 and H3 compounds against the HT-29 cancer cell line was studied. The anti-proliferative activity of H2 and H3 was tested by examining their ability to inhibit cell proliferation. The results demonstrated that H2 and H3 have a highly cytotoxic effect against the HT-29 cell line.as shown in Fig. 9. The cytotoxicity of H2 and H3 was found to be concentration and time-dependent. The cytotoxic effect and morphological changes were observed in the HT-29 cells after treatment with concentrations of 12.50, 25, 50,

Parameters	H2	H3
Physicochemical properties		
Molecular weight (Da)	279.29 g/mol	269.32 g/mol
Log Po/w (MLOGP)	1.6	1.77
Number of H-bond acceptors	3	2
Number of H-bond donors	3	2
Molar refractivity	81.49	77.34
Number of rotatable bonds	4	4
TPSA (Å2)	77.48 Å²	88.49 Å²
Pharmacokinetics		
Gastrointestinal (GI) absorption	High	High
Blood-brain barrier	No	No
(BBB) permeant	Yes	Yes
P-glycoprotein substrate	No	No
Log Kp (skin permeation)	– 6.16 cm/s	– 5.83 cm/s
Drug likeness		
Log S (ESOL)	– 3.47	– 3.66
Water solubility class	Moderately soluble	Moderately soluble
Lipinski rule	Yes; 0 violation	Yes; 0 violation
Ghose	Yes	Yes
Veber	Yes	Yes
Egan	Yes	Yes
PAINs	Yes	Yes
Bioavailability score	0.55	0.55
Metabolism		
CYP1A2 inhibitor	Yes	Yes
CYP2C19 inhibitor	No	No
CYP2C9 inhibitor	No	No
CYP2D6 inhibitor	No	No

Table 2. ADMET Protocol and drug-likeness properties of the (H2 and H3) compounds.

Bonds between compound atoms and 7ZWA active site residues									
Compd.	Score (kcal/mol)	RMSD (Å)	Compd. atoms	Receptor atoms	Receptor residues	Interaction	d (Å)	E (kcal/mol)	Total E (kcal/mol)
H2	− 5.6203	1.8083	N 16	OE1	GLU 250 (A)	H-donor	3.14	− 4.1	− 30.860
			O 32	O	GLU 250 (A)	H-donor	2.95	− 1.4	
			N 16	OD2	ASP 81 (A)	Ionic	3.16	− 3.5	
			N 16	OE1	GLU 250 (A)	Ionic	3.14	− 3.6	
H3	− 5.4409	1.6738	S 28	OD1	ASP 79 (A)	H-donor	3.95 3.80	− 1.3	− 30.1819
			S 28	OD2	ASP 79 (A)	H-donor	2.95	− 0.5	
			O 21	NE	ARG 252 (A)	H-acceptor	3.95 3.80	− 3.4	

Table 3. Valid molecular docking scores were found between the H2 and H3 compounds under study and the amino acids of *colorectal cancer (CRC)* (ID: 7ZWA). Additionally, binding affinity and RMSD were also demonstrated for the compounds.

100, and 200 µg mL^{-1} of H2 and H3. The H3 compound had more activity against the HT-29 cell line, especially when using a higher concentration of H3 (200 µg mL^{-1}) with an increase in time. The results of the present study established that the treatment of H2 and H3 inhibits the development of cancer cells in a dose-dependent manner and over time (24, 48, and 72 h). The 3-(4,5-dimethylthiazol-2-yl)-2,5-diphenyl tetrazolium bromide (MTT) cell viability assay is a widely used colorimetric test to determine cell viability or cytotoxicity. The study suggests that the cytotoxic effect of H2 and H3 against HT-29 cancer cells may involve a variation of cell signaling pathways, but the exact mechanism of action is not completely known and requires further investigation. Using the MTT assay, the antiproliferative activity of the new N-acyl hydrazones was assessed on the prostate (PC-3) and breast (MCF-7) cancer cell lines. Furthermore, normal cells of breast epithelial cells (ME-16 C) were tested. Compounds 7a-e, 8a-e, and 9a-e, shown specific antiproliferative action and substantial toxicity to both cancer cells at the same time, while showing no damage to normal cells. From these new N-acyl hydrazones, 7a-e exhibited the strongest antitumor effects, with IC50 values against MCF-7 and PC-3 cells of 7.52 ± 0.32–

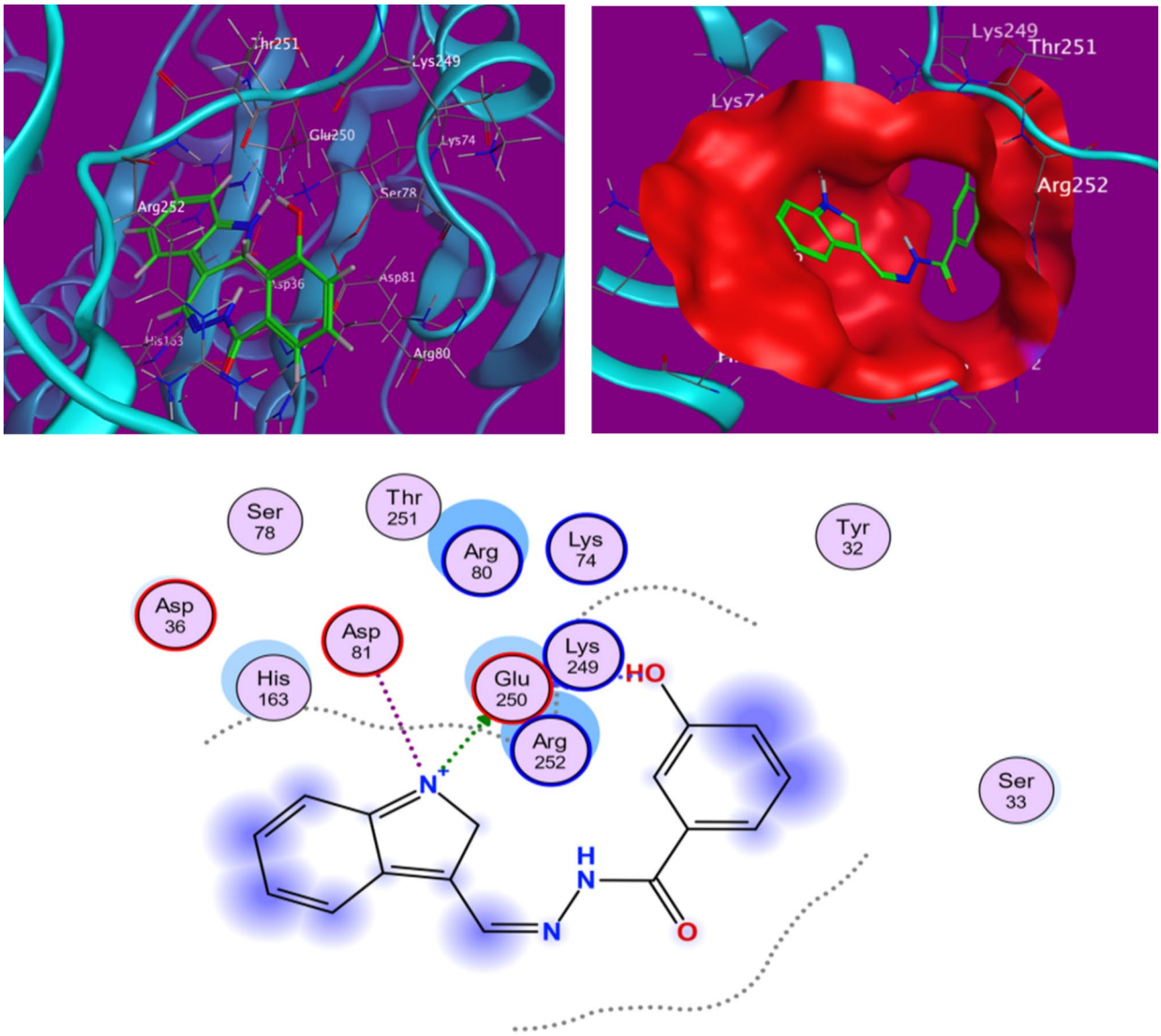

Fig. 6. H-bond distances and 3D and 2D interactions between the investigated, H2, compounds and the amino acids of colorectal cancer (CRC) (ID: 7ZWA).

25.41 ± 0.82 and 10.19 ± 0.52–57.33 ± 0.92 μM, respectively. Additionally, to understand possible molecular interactions between drugs and target proteins, molecular docking experiments were used. It was observed that there is good agreement between the experimental results and the docking calculations[34]. Four compounds with a diphenylamine moiety containing pyrrolidinone-hydrazone derivatives were found to be anticancer agents. With IC_{50} values between 2.5 and 20.2 μM, these compounds showed the greatest selectivity against the prostate cancer cell line PPC-1 and the melanoma cell line IGR39. None of the drugs demonstrated an inhibitory effect on the migration of the triple-negative breast cancer MDA-MB-231 cell line, and they were less effective against this cell type. The most promising derivative that might be further developed as an antimetastatic agent was found to be N′-((5-nitrothiophen-2-yl)methylene)-5-oxo-1-(4-(phenylamino)phenyl)pyrrolidine-3-carbohydrazide in the wound healing assay. In IGR39 cell spheroids, N′-(5-chloro- and N′-(3,4-dichlorobenzylidene)-5-oxo-1-(4-(phenylamino)phenyl)pyrrolidine-3-carbohydrazides were the most effective in reducing cell survival. On PPC-1 3D cell cultures. However, pyrrolidinone-hydrazone derivatives had no effect[35]. In the recent published study[36], they designed and assessment of a number of new Tetracaine derivatives with hydrazide-hydrazone moiety for their potential anticancer properties. FT-IR, 13 C NMR, 1 H NMR, and HRMS techniques were used to analyze the spectrum properties of these compounds. All manufactured compounds were examined for its ability to inhibit cancer growth using two distinct human cancer cell lines, namely Colo-205 and HepG2. Compounds 2f and 2 m exhibited the strongest anticancer activity against the Colo-205 cell line ($IC_{50} = 50.0$ and 20.5 μM, respectively) out of all the produced chemicals. The compounds with the greatest anticancer activity against the HepG2 cell line were 2k, 2p, and 2s (IC50 = 30.5, 35.9, and 20.8 μM, respectively).

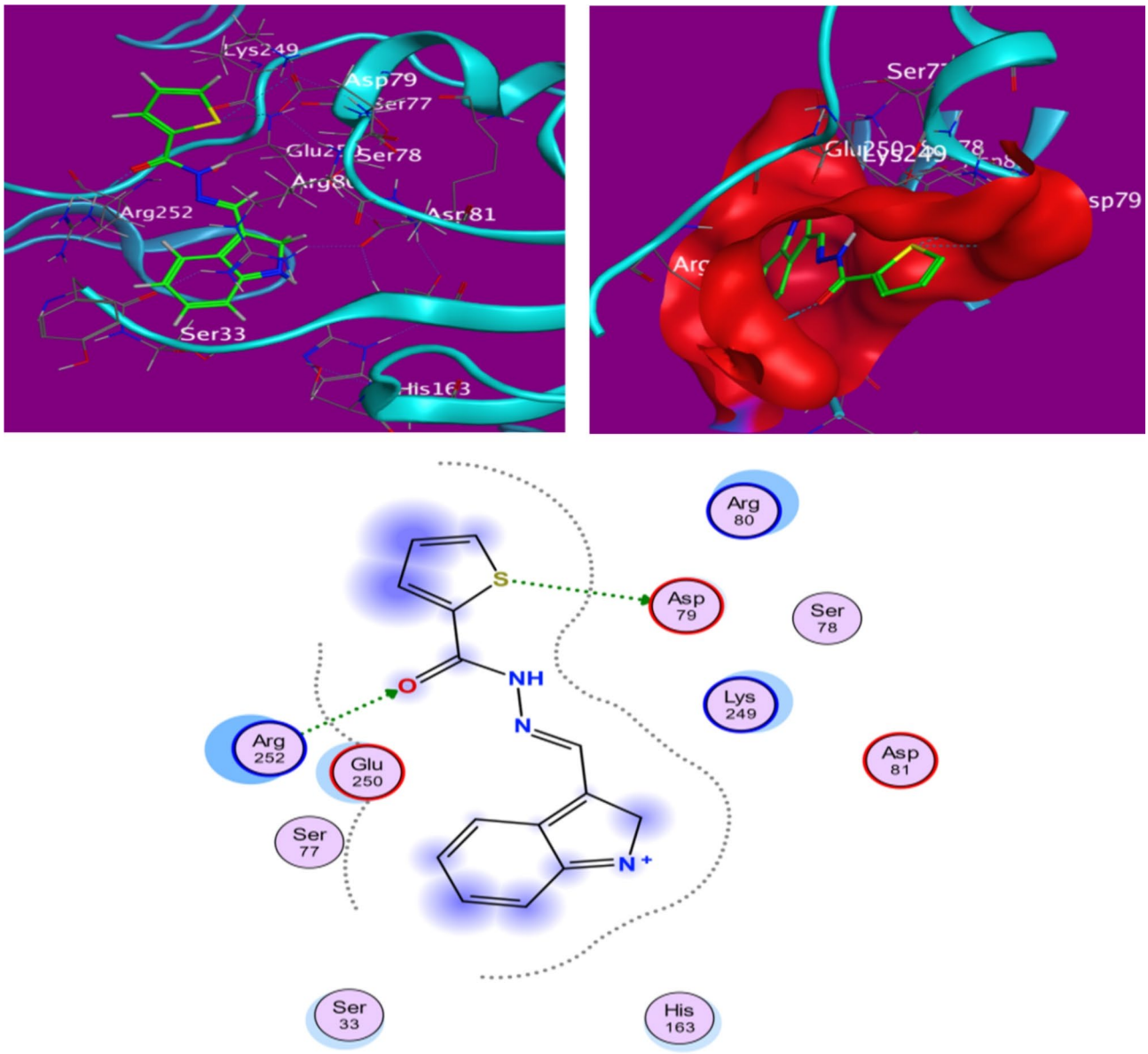

Fig. 7. H-bond distances and 3D and 2D interactions between the investigated, H3, compounds and the amino acids of colorectal cancer (CRC) (ID: 7ZWA).

H2 and H3 induced HT-29 cell death

The ability of H2, and H3 to induce apotosis in HT-29 cells is indicated in Fig. 10. Apoptosis, the highly regulated process of programmed cell death, involves the control of various cellular signaling proteins[37]. The dual staining method using Acridine Orange (AO) and Ethidium Bromide (EtBr) fluorescent dyes was employed to observe and quantify the changes related to apoptosis in the HT-29 cell line, both in the control and H2/H3-treated samples. Normal or viable cells typically exhibit organized green fluorescence, while early apoptotic cells show bright green, and late apoptotic cells display red-orange fluorescence due to their damaged, condensed, and fragmented chromatin[38]. The fluorescence imaging in Fig. 10 illustrates the observations. Figure 10A shows the untreated HT-29 cells, appearing green. Figure 10B depicts the HT-29 cells treated with the H2 drug concentration, exhibiting yellow-green color with signs of DNA damage and fragmentation, indicating partial apoptosis. Figure 10C shows the H3-treated HT-29 cells with orange-red fluorescence, suggesting EtBr penetration and late-stage apoptosis, indicating advanced apoptosis. In the study of[36], using both Colo-205 and HepG2 cell lines, real-time polymerase chain reaction (qRT-PCR) analysis was used to measure the mRNA transcription levels of the Bax and caspase-3 genes. The reference standard for positive sensitivity was doxorubicin. A time-dependent increase in the expression levels of Bax and Caspase 3 on apoptosis was demonstrated by qRT-PCR analysis. Western blotting was used to examine the inhibition of apoptotic proteins PI3K, Akt, PTEN, pPTEN, FoXO1, FoXO3a, TXNIP, and p27 in Colo-205 and HepG2 cells treated with chemicals 2f, 2 m, 2k, 2p, and 2s. The three breast cancer cell lines (MCF-7, MDA MB-231, and MDA MB-468) were used to test the novel 2 H-chromene-based

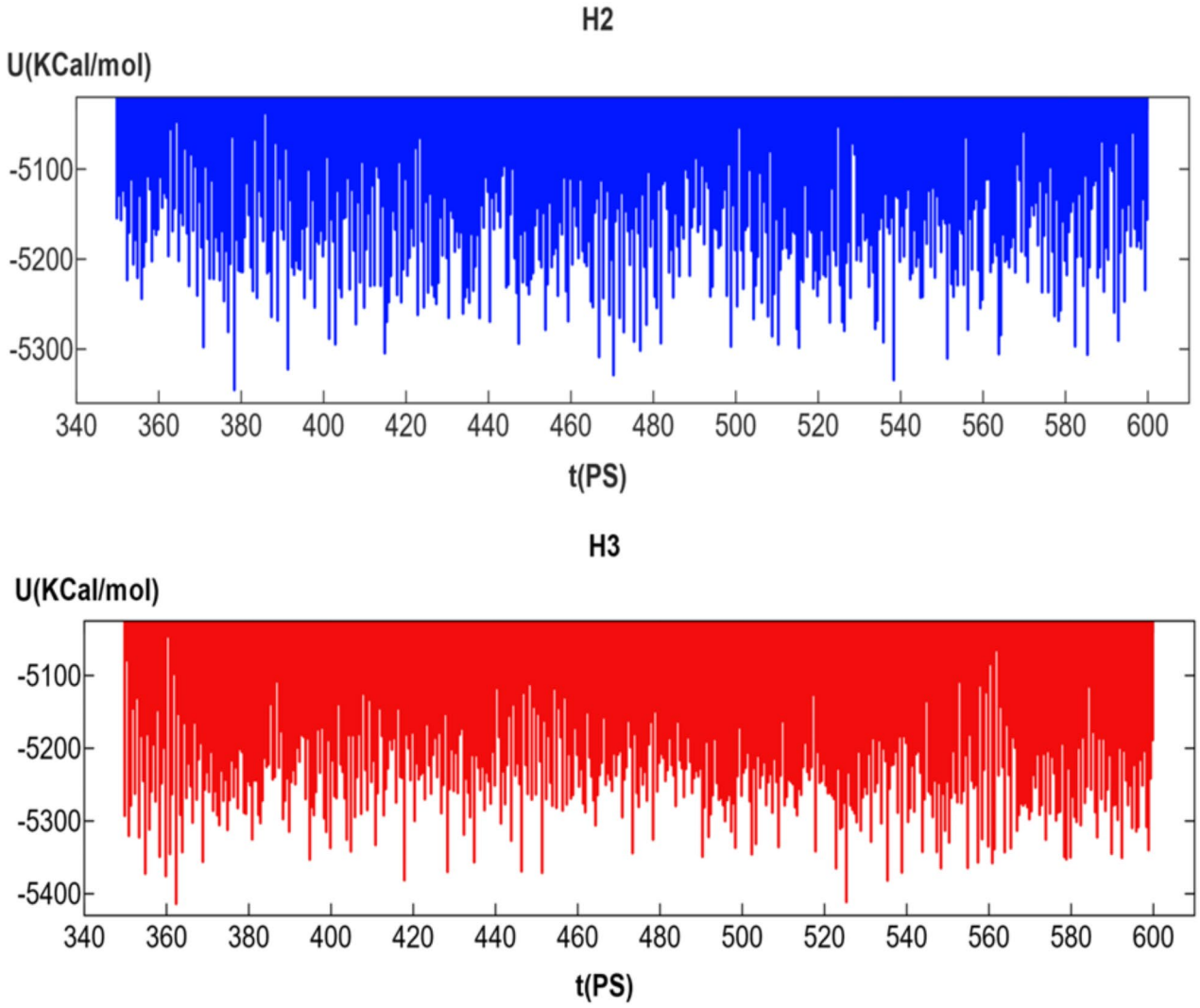

Fig. 8. MD simulation of each (H2, and H3) compound and its behavior on *colorectal cancer (CRC)* amino acids (ID: 7ZWA).

hydrazones' in vitro anticancer activities using the MTT assay. Among the produced compounds, compounds 10 r and 12 b shown the most antiproliferative activity against MCF-7 cell, with IC50 values of 9.12 ± 0.45 μM and 10.71 ± 0.67 μM, respectively. According to flow cytometric analysis, these two powerful substances, 10 r and 12 b, caused dose-dependent protein apoptosis and stopped the cell cycle at the G2/M phase. Annexin V-FITC test and Hoechst staining provided additional confirmation. Furthermore, in silico molecular docking analysis of compounds 10 r and 12 b demonstrated that compound 10 r had a good binding affinity energy of around −10 kcal/mol with the human HER2 receptor. Additionally, the hybrid compounds exhibiting encouraging physicochemical, pharmacokinetic, and drug-like properties were verified by the ADME studies[39].

Conclusion

New compounds, namely, 3-hydroxybenzohydrazide [H1], (E)-N'-((1H-indol-3-yl)methylene)-3-hydroxybenzohydrazide [H2], and (E)-N'-((1H-indol-3-yl)methylene)thiophene-2-carbohydrazide [H3], were successfully synthesized using conventional methods. The characterization of these compounds (H1, H2, and H3) was performed with different spectroscopic techniques (FT-IR, ^{1}H-NMR, and ^{13}C-NMR) .The produced substances H2 and H3 exhibited notable antioxidant, antifungal, and antibacterial properties. The compound H3 revealed high activity against Staphylococcus aureus bacteria. By adding substituents at different points along the Schiff base core, significant positive results in antimicrobial activity screening were obtained in the structure-activity study on Schiff base derivatives. Therefore, it is imperative to carry out research on the synthesis of new antimicrobial compounds by incorporating appropriate functional groups into different sites surrounding the Schiff base core. As an apoptotic inducer and antiproliferative against *Staphylococcus aureus* bacteria, compound H3 was found to be highly effective. Because of the importance of synthetic compounds, the application of density functional theory, ADMET studies, molecular docking, and molecular dynamics simulations to the H2

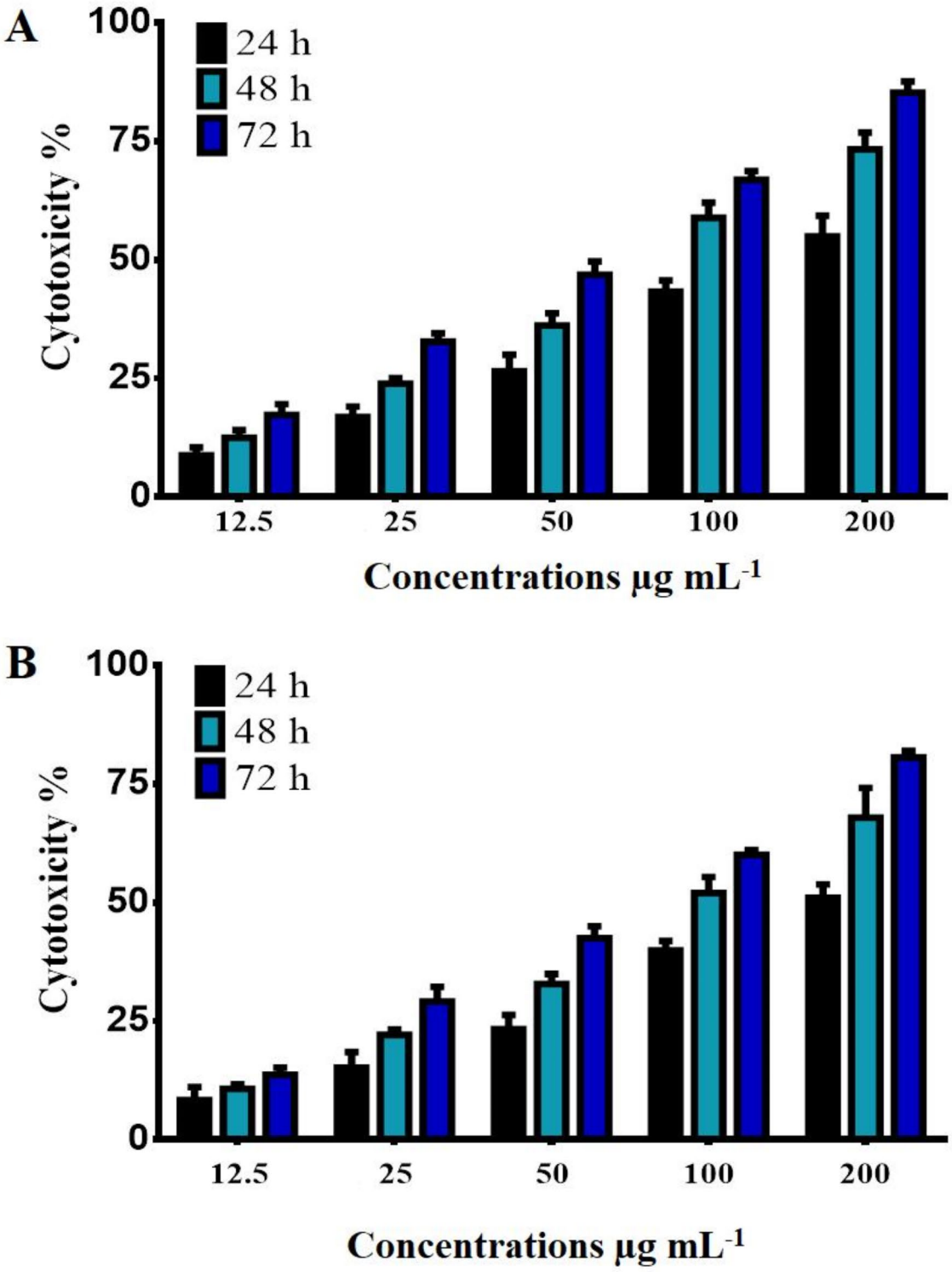

Fig. 9. Cytotoxicity effect of (**A**) H2 and (**B**) H3 in HT-29 cells.

and H3 compounds can provide comprehensive insights into their chemical and biological properties. These techniques collectively aid in assessing the viability of H2 and H3 as drug candidates, optimizing their structures for better efficacy and safety, and predicting their behavior within biological systems.

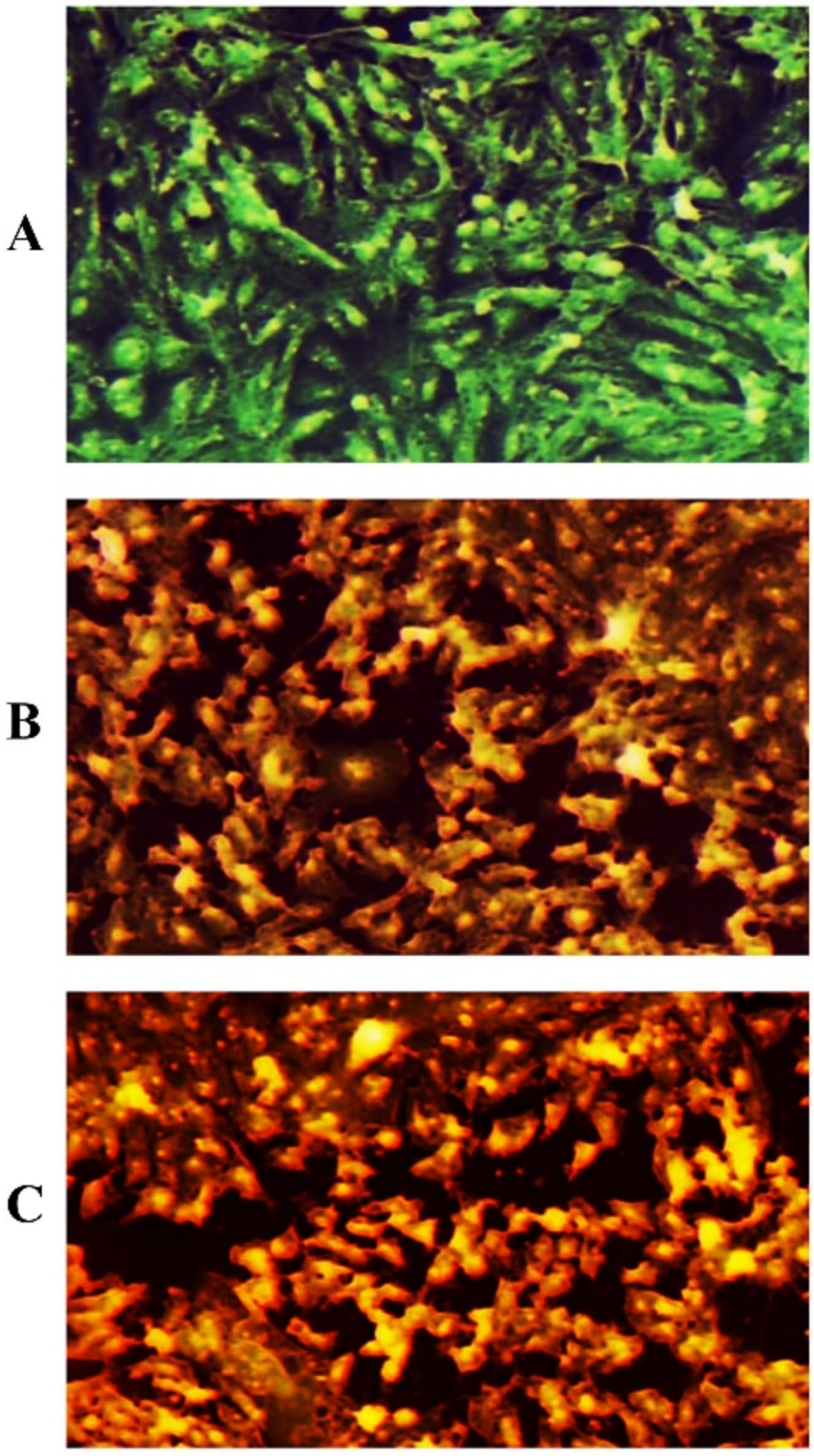

Fig. 10. Apoptosis markers in HT-29 cells following treatment with H2, and H3. (**A**) Control untreated HT-29 cells. (**B**) HT-29 cells after been treated with H2. (**C**) HT-29 cells after been treated with H3.

Data availability

Molecular docking and molecular dynamic simulation study using the program (https://www.chemcomp.com/en/Products.htm). The protein structure used in the present study, obtained from the PDB (Protein Data Bank), is available at (https://www.rcsb.org/structure/7ZWA). ADMET Protocol and Drug-Likeness Prediction using (http://www.swissadme.ch/). Quantum and reactivity parameters using (https://gaussian.com/). The structures

of compounds were drawn using Chem Office (15.0) (https://perkinelmer-chemoffice-professional.software.informer.com/15.0/#google_vignette).

Received: 12 September 2024; Accepted: 27 November 2024
Published online: 02 December 2024

References

1. Priya, B., Utreja, D., Sharma, S., Kaur, G. & Madhvi. Synthesis and antimicrobial activities of indole-based Schiff bases and their metal complexes: a review. *Curr. Org. Chem.* **27**, 941–961. https://doi.org/10.2174/1385272827666230901140611 (2023).
2. Ibraheem, H. H., Issa, A. A. & El-Sayed, D. S. Structural behavior and surface layer modification of (E)-N'-((1H-indol-3-yl) methylene)-4-chlorobenzohydrazide: Spectroscopic, DFT, biomedical activity and molecular dynamic simulation against Candida Albicans receptor. *J. Mol. Struct.* **1312**, 138484. https://doi.org/10.1016/j.molstruc.2024.138484 (2024).
3. Adel, M. H. & Ibraheem, H. Synthesis, molecular docking, and anti-tumor activity of pyrazole derivatives. In Fifth International Conference on Applied Sciences: ICAS2023. (2023)., December https://doi.org/10.1063/5.0210692
4. Jima'a, R. B. & Shaalan, N. D. Synthesis, characterization, and biological activity of new metal ion complexes with Schiff base derived from 2-acetylthiophene and isatin. *Egypt. J. Chem.* https://doi.org/10.21608/EJCHEM.2022.124768.5552 (2022).
5. AL-Hashemmi, A. & Farhan, M. S. Synthesis, identification and preliminary pharmacological evaluation of new hydrazone and 1, 3, 4-oxadiazole derivatives of ketorolac. *Iraqi J. Pharm. Sci.* **33** (1), 113–122. https://doi.org/10.31351/vol33iss1pp113-122 (2024).
6. Ibrahim, J. A., Ibraheem, H. H. & Hussein, H. T. Experimental and theoretical studies on the corrosion inhibition potentials of N'-(1H-indole-3-yl)methylene)benzohydrazide for mild steel in HCl. *Int. J. Corros. Scale Inhib.* **13** (1), 94–120. https://doi.org/10.17675/2305-6894-2024-13-1-6 (2024).
7. Issa, A. A. et al. Nanocluster-based computational creation of a potential carrier for chemotherapeutic antibacterial drugs. *J. Inorg. Organomet. Polym. Mater.* 1–16. https://doi.org/10.1007/s10904-024-03116-1 (2024).
8. Mahmood, W. K., Dakhal, G. Y., Younus, D., Issa, A. A. & El-Sayed, D. S. Comparative properties of ZnO modified Au/Fe nanocomposite: electronic, dynamic, and locator annealing investigation. *J. Mol. Model.* **30**, 165. https://doi.org/10.1007/s00894-024-05956-7 (2024).
9. Ibraheem, H. H., Shubrem, A. S., Al-Majedy, Y. K. & Issa, A. A. Experimental studies on the corrosion inhibition performance of chalcone derivative for mild steel in acid and alkaline solution, in: : p. 030044. (2022). https://doi.org/10.1063/5.0091889
10. Issa, A. A., Kamel, M. D., & El-Sayed, D. S. Depicted simulation model for removal of second-generation antipsychotic drugs adsorbed on Zn-MOF: adsorption locator assessment. *J. Mol. Model.* **30**, 106. https://doi.org/10.1007/s00894-024-05896-2 (2024).
11. Al-Majedy, Y. K., Ibraheem, H. H. & Issa, A. A. Antioxidant, antimicrobial activity and quantum chemical studies of 4-methyl-7-hyroxy coumarin derivatives, in: : p. 060002. (2023). https://doi.org/10.1063/5.0113038
12. Al-Majedy, Y. K., Ibraheem, H. H., Issa, A. A., & Alamiery, A. Exploring chromone derivatives. As environmentally friendly corrosion inhibitors for mild steel in acidic environments: a comprehensive experimental and DFT study. *Int. J. Corros. Scale Inhib.* **12** https://doi.org/10.17675/2305-6894-2023-12-3-14 (2023).
13. Jabbar, A. & Al-Majedy, Y. K. Multi-faceted investigation: DFT studies and corrosion inhibition potential of 4-(2-((2-methyl-1H-indol-3-yl)methylene)hydrazinyl)-phenol for mild steel in 0.5 M HCl medium. *Int. J. Corros. Scale Inhib.* **13** (2), 790–811. https://doi.org/10.17675/2305-6894-2024-13-2-8 (2024).
14. Maniak, H., Talma, M., Matyja, K., Trusek, A. & Giurg, M. Synthesis and structure-activity relationship studies of Hydrazide-hydrazones as inhibitors of laccase from Trametes Versicolor. *Molecules* **25**, 1255. https://doi.org/10.3390/molecules25051255 (2020).
15. Hassan, M. A. et al. The synergistic influence of polyflavonoids from Citrus aurantifolia on Diabetes Treatment and their modulation of the PI3K/AKT/FOXO1 signaling pathways: molecular docking analyses and in vivo investigations. *Pharmaceutics* **15.** https://doi.org/10.3390/pharmaceutics15092306 (2023).
16. Feng, Y., Zhang, Y. & Ebright, R. H. Structural basis of transcription activation. *Sci. (80-).* **352**, 1330–1333. https://doi.org/10.1126/science.aaf4417 (2016).
17. Kadhim, R. J., Karsh, E. H., Taqi, Z. J. & Jabir, M. S. Biocompatibility of gold nanoparticles: In-vitro and In-vivo study. *Mater. Today: Proc.* **42**, 3041–3045 (2021).
18. Abbas, Z. S. et al. Galangin/β-Cyclodextrin inclusion complex as a drug-delivery system for Improved solubility and biocompatibility in breast Cancer Treatment. *Molecules* **27** (14), 4521 (2022).
19. Sameen, A. M., Jabir, M. S. & Al-Ani, M. Q. Therapeutic combination of gold nanoparticles and LPS as cytotoxic and apoptosis inducer in breast cancer cells. In *AIP Conference*.
20. Elshibani, F. A. et al. Phytochemical and biological activity profiles of Thymbra linearifolia: an exclusively native species of Libyan green mountains. *Arab. J. Chem.* **16**, 104775. https://doi.org/10.1016/j.arabjc.2023.104775 (2023).
21. Agili, F. Novel hydrazide hydrazone derivatives as Antimicrobial agents: design, synthesis, and Molecular Dynamics. *Processes* **12** (6), 1055 (2024).
22. Ramalho, T. C., Caetano, M. S., da Cunha, E. F. F., Souza, T. C. S. & Rocha, M. V. J. Construction and Assessment of reaction models of Class I EPSP synthase: Molecular Docking and Density Functional theoretical calculations. *J. Biomol. Struct. Dyn.* **27**, 195–207. https://doi.org/10.1080/07391102.2009.10507309 (2009).
23. Sturgeon, J. B. & Laird, B. B. Symplectic algorithm for constant-pressure molecular dynamics using a Nosé–Poincaré thermostat. *J. Chem. Phys.* **112**, 3474–3482. https://doi.org/10.1063/1.480502 (2000).
24. Aslanhan, Ö., Kalay, E., Tokalı, F. S., Can, Z. & Şahin, E. Design, synthesis, antioxidant and anticholinesterase activities of novel isonicotinic hydrazide-hydrazone derivatives. *J. Mol. Struct.* **1279**, 135037 (2023).
25. Shaker, L. M. et al. An overview of the density functional theory on antioxidant bioactivity predictive feasibilities: insights from natural antioxidant products. *J. Mol. Struct.* **1301**, 137393. https://doi.org/10.1016/j.molstruc.2023.137393 (2024).
26. Ibraheem, H., Al-Majedy, Y., Issa, A. A. & Yousif, E. Photostabilization, thermodynamic and theoretical studies of polystyrene by some 2-amino pyridine. *Trends Sci.* **21**, 7374. https://doi.org/10.48048/tis.2024.7374 (2023).
27. Shakir, S. M., & Al-Majedy, Y. K. Synthesis Bio-evaluation and Quantum Chemical Studies of some coumarin derivatives. *J. Appl. Sci. Nanotechnol* **2**(1), (2022).
28. Mohammed, H.A. et al. Chrysin, the Flavonoid molecule of antioxidant interest. *ChemistrySelect* **8**, 1–15. https://doi.org/10.1002/slct.202303306 (2023).
29. Roussaki, M., Kontogiorgis, C. A., Hadjipavlou-Litina, D., Hamilakis, S. & Detsi, A. A. Novel synthesis of 3-Aryl coumarins and evaluation of their antioxidant and lipoxygenase inhibitory activity. *Bioorg. Med. Chem. Lett.* **20** (13), 3889–3892 (2010).
30. Valko, M. et al. Free radicals and antioxidants in normal physiological functions and human disease. *Int. J. Biochem. Cell. Biol.* **39** (1), 44–84 (2007).
31. Al-Duhaidahawi, D. L., Al-Majedy, Y. K., Ibraheem, H. H., Kadhum, A. A. H. & Al-Amiery, A. A. Macro coumarins as Novel antioxidants. *Orient. J. Chem.* **34** (5), 2562 (2018).
32. Bhatia, R. K. et al. Novel P-Functionalized Chromen-4-on-3-Yl Chalcones Bearing Astonishing Boronic Acid Moiety as MDM2 inhibitor: synthesis, cytotoxic evaluation and Simulation studies. *Med. Chem. (Los Angeles).* **16** (2), 212–228 (2020).

33. Daoui, O. et al. Molecular Docking and ADMET properties in Silico studies of Novel 4, 5, 6, 7-Tetrahydrobenzo [D]-Thiazol-2-Yl derivatives derived from Dimedone as Potent Anti-tumor agents through inhibition of C-Met receptor tyrosine kinase. *Heliyon* **7**, 7 (2021).
34. Biliz, Y. et al. Novel N-acyl hydrazone compounds as promising anticancer agents: synthesis and molecular docking studies. *ACS Omega*. **8** (22), 20073–20084 (2023).
35. Zubrickė, I., Jonuškienė, I., Kantminienė, K., Tumosienė, I. & Petrikaitė, V. Synthesis and in vitro evaluation as potential anticancer and antioxidant agents of diphenylamine-pyrrolidin-2-one-hydrazone derivatives. *Int. J. Mol. Sci.* **24** (23), 16804 (2023).
36. Han, M. İ. & Imamoglu, N. Design, synthesis, and anticancer evaluation of novel tetracaine hydrazide-hydrazones. *ACS Omega*. **8** (10), 9198–9211 (2023).
37. Chen, Y., Li, X., Yang, M. & Liu, S. B. Research progress on morphology and mechanism of programmed cell death. *Cell Death Dis.* **15** (5), 327 (2024).
38. Oh, S. J. et al. Incompatibility of silver nanoparticles with lactate dehydrogenase leakage assay for cellular viability test is attributed to protein binding and reactive oxygen species generation. *Toxicology Letters.* **225**(3), 422–432 (2014).
39. Shankar Panda, B. et al. New 2H-Chromene-Based Hydrazone Derivatives as Promising Anti-Breast Cancer Agents: Efficient Synthesis, Spectral Characterization, Molecular Docking, and ADMET Studies. *Chemistry Select.* **9**(15), e202400115.

Acknowledgements
The authors extend their appreciation to the Researchers Supporting Project number (RSPD2024R971), King Saud University, Riyadh, Saudi Arabia for funding this research.

Author contributions
Conceptualization and methodology; Hiba H. Ibraheem, Batool K. Queen, Matheel D. Al-Sabti, Ali A. Issa, Majid S. Jabir, Ghassan M. Sulaiman; Formal analysis, Ghassan M. Sulaiman, Majid S. Jabir; Investigation and data curation, Ghassan M. Sulaiman , Majid S. Jabir; validation, Mazin A. A. Najm, Ayman A. Swelum; visualization, Buthenia A. Hasoon, Merriam M. Eshaq, Yasameen K. Al-Majedy, Kareem H. Jawad Original draft preparation, Buthenia A. Hasoon, Merriam M. Eshaq, Yasameen K. Al-Majedy, Kareem H. Jawad, Sabrean F. Jawad, Hayder A. Fawzi, Muhammad Shuaib; writing—review and editing; Hiba H. Ibraheem, Ali A. Issa, Majid S. Jabir, Ghassan M. Sulaiman. All authors reviewed the manuscript.

Funding
The authors extend their appreciation to the Researchers Supporting Project number (RSPD2024R971), King Saud University, Riyadh, Saudi Arabia for funding this research.

Declarations

Competing interests
The authors declare no competing interests.

Additional information
Supplementary Information The online version contains supplementary material available at https://doi.org/10.1038/s41598-024-81555-z.

Correspondence and requests for materials should be addressed to M.S.J., G.M.S. or A.A.S.